Journal of Applied Polymer Science

Preparation of glucose-sensitive and fluorescence micelles via a combination of photoinitiated polymerization and chemoenzymatic transesterification for the controlled release of insulin

Xiangxiang Du,[1] Guohua Jiang,[1,2,3] Lei Li,[1] Wentong Yang,[4] Hua Chen,[1] Yongkun Liu,[1] Qin Huang[1]

[1]Department of Materials Engineering, Zhejiang Sci-Tech University, Hangzhou 310018, People's Republic of China

[2]National Engineering Laboratory for Textile Fiber Materials and Processing Technology (Zhejiang), Hangzhou 310018, People's Republic of China

[3]Key Laboratory of Advanced Textile Materials and Manufacturing Technology, Ministry of Education, Hangzhou 310018, People's Republic of China

[4]Qixin Honours School, Zhejiang Sci-Tech University, Hangzhou 310018, People's Republic of China

Correspondence to: G. Jiang (E-mail: ghjiang_cn@zstu.edu.cn)

ABSTRACT: Glucose-sensitive and fluorescence copolymer micelles were designed and prepared via a combination of photoinitiated polymerization and enzymatic transesterification. The water-soluble photoinitiator and emulsifier 2-oxooctanoic acid self-polymerized dimer molecules under UV irradiation were characterized by mass spectrometry. The fluorescence dye (9-anthracene alcohol) and biocompatible hydrophilic chains [poly(ethylene glycol)] were introduced to the polymer chains during the photopolymerization and enzymatic transesterification processes. The as-prepared copolymers were confirmed by ^{1}H-NMR spectroscopy, Fourier transform infrared spectroscopy, transmission electron microscopy, and dynamic light scattering. The resulting copolymers exhibited excellent glucose sensitivity and stability against protein. The optical fluorescence properties of the copolymer micelles were investigated with fluorescence spectrophotometry, fluorescence microscopy, and confocal laser scanning microscopy. Because of the amphiphilic feature, the micelles could be self-assembled and used to load insulin. The controlled release of insulin was evaluated and was triggered by glucose *in vitro*. This study provided a new strategy for fabricating functional carriers as self-regulated insulin-release systems. © 2015 Wiley Periodicals, Inc. J. Appl. Polym. Sci. **2016**, *133*, 43026.

KEYWORDS: biomaterials; drug-delivery systems; emulsion polymerization; photopolymerization

Received 12 July 2015; accepted 7 October 2015

DOI: 10.1002/app.43026

INTRODUCTION

In recent years, smart drug-delivery systems have received much attention because of the controlled drug release triggered by external stimuli, such as the pH,[1,2] temperature,[3,4] light,[5,6] glucose,[7,8] and CO_2.[9,10] Among these stimuli-sensitive polymeric drug carriers, glucose-sensitive polymeric drug-delivery vehicles have been investigated for potential biomedical applications in glucose biosensors and detection, glucose-triggered release systems, and the treatment of diabetes.[11–13] With the rapid development of modern imaging technology, fluorescence-polymer-based biomaterials make possible their detection for imaging purposes applied in the biological field by common optical systems, such as cell imaging and drug-release monitoring.[14–17] Thus, it is greatly significant to prepare glucose-sensitive fluorescent amphiphilic polymer insulin carriers; this is promising for providing a diabetes therapy approach. To this point, most research involved with polymer-based drug-carrier preparation methods have focused on radical thermally initiated polymerization,[18,19] ring-opening polymerization,[20,21] atom transfer radical polymerization,[22,23] reversible addition–fragmentation chain-transfer polymerization,[24,25] and living ionic polymerization,[26,27] either by the copolymerization of monomers or through postpolymerization functionalization. However, they inevitably use organic solvents, initiators, and/or surfactants. Self-emulsifying photoinitiating radical systems provide facile, simple, economic methods.[28–30] It is a good strategy to obtain block or graft polymers with water-soluble photoinitiators; this produces free-radical intermediates on irradiation with low activation energies at room temperature. As is known to all, enzymes are mild, efficient catalysts. The expected functional groups, such as fluorescence groups, can be introduced into specific molecular sites with specific enzymes.[31,32] To the best of our

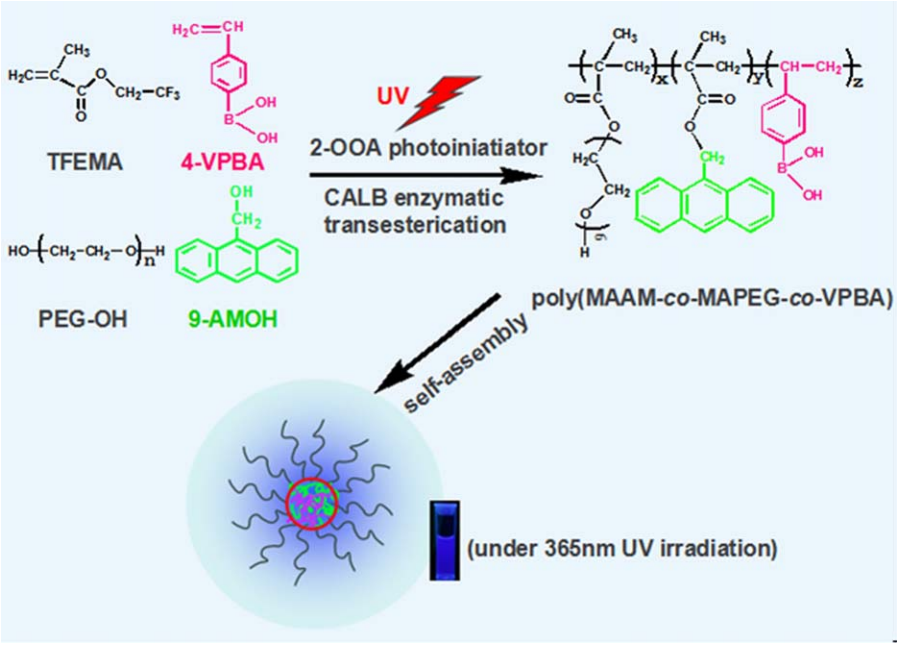

Scheme 1. Synthetic route of the poly(MAAM-*co*-MAPEG-*co*-VPBA) copolymer via the photoinitiated polymerization and enzymatic transesterification combination method. [Color figure can be viewed in the online issue, which is available at wileyonlinelibrary.com.]

knowledge, there are limited reports on the combination of photoinitiated and chemoenzymatic transesterification polymerizations for the preparation of glucose-sensitive fluorescent amphiphilic polymers.

Herein, glucose-sensitive and fluorescent amphiphilic copolymers were synthesized by a combination of photoinitiated polymerization and enzymatic transesterification in the presence of water-soluble 2-oxooctanoic acid (2-OOA). Because of the photolysis of 2-OOA under UV irradiation, the dimer molecules acted as the surfactant or emulsifier to form micelles in solution. The free radicals formed by the photolysis procedure were dissociated in solution to initiate the polymerization of 4-vinyl phenyl boronic acid (4-VPBA) and trifluoroethyl methacrylate (TFEMA) monomers. The fluorescence label [9-anthracene alcohol (9-AMOH)] and biocompatible hydrophilic chains [poly(ethylene glycol) (PEG-OH)] were introduced to functionalize the micelles by chemoenzymatic (Candida antarctica lipase B (CALB) enzyme) transesterification, as shown in Scheme. 1. Insulin was loaded into the glucose-sensitive and fluorescent amphiphilic polymers for the simulation of drug release. The release of insulin was triggered by glucose. In addition, the cytocompatibility experiment was carried out to evaluate potential biomedical applications by methyl thiazolyl tetrazolium (MTT) analysis.

EXPERIMENTAL

Materials

2-OOA (99%) was purchased from Shanghai Energy Chemical Co. (China). TFEMA [analytical reagent (AR)], 4-VPBA (AR), 9-AMOH (98%), PEG-OH (average molecular weight $M = 400$), insulin (derived from pig pancreas, ≥ 27 IU mg^{-1}), and *N*,*N*-dimethylformamide (AR) were purchased from Shanghai Aladdin Reagent Co., Ltd. (China). CALB enzyme was purchased from Beijing Cliscent Science and Technology Co., Ltd. (China). All other chemicals and solvents were analytical grade and were used without further purification.

2-OOA Self-Polymerization under UV Irradiation

An amount of 15 mg of 2-OOA was dissolved 10 mL of deionized water with sonication until the solution became transparent, and then, the previously obtained solution was transferred to a flask. The flask was immersed in liquid nitrogen and was followed by three freeze–pump–thaw cycles. The final solution preparation was done under UV irradiation.

Synthesis of the Poly(methacrylate anthracene methyl-*co*-methacrylate poly(ethylene glycol)-*co*-vinyl phenyl boronic acid)(poly(MAAM-*co*-MAPEG-co-VPBA) Copolymer

The poly(MAAM-*co*-MAPEG-*co*-VPBA) copolymers were prepared via photoinitiated polymerization and chemoenzymatic transesterification. First, 10 mg of 2-OOA was dissolved in 15 mL of deionized water with sonication until the solution became transparent. Then, 0.1054 g (0.625 mmol) of TFEMA, 0.08 g of CALB enzyme, 0.2260 g (0.565 mmol) of PEG-OH, 0.0131 g (0.0625 mmol) of 9-AMOH, and 0.0745 g (0.503 mmol) of 4-VPBA dissolved in 0.2 mL of *N*,*N*-dimethylformamide were added to the previous transparent solution with vigorous stirring until the solution became opalescent. The previous solution was transferred to a reaction flask and then immersed in liquid nitrogen; this was followed by three freeze–pump–thaw cycles. The opalescent solution was reacted under UV irradiation for 5 h. The obtained product was dialyzed against deionized water for 3 days with a dialysis bag with a molecular cutoff (MWCO) of 3500 Da. The final product was lyophilized to obtain a yellowish powder.

In the control experiment, poly(trifluroethyl methacrylate-*co*-vinyl phenyl boronic acid) poly(TFEMA-*co*-VPBA) was prepared

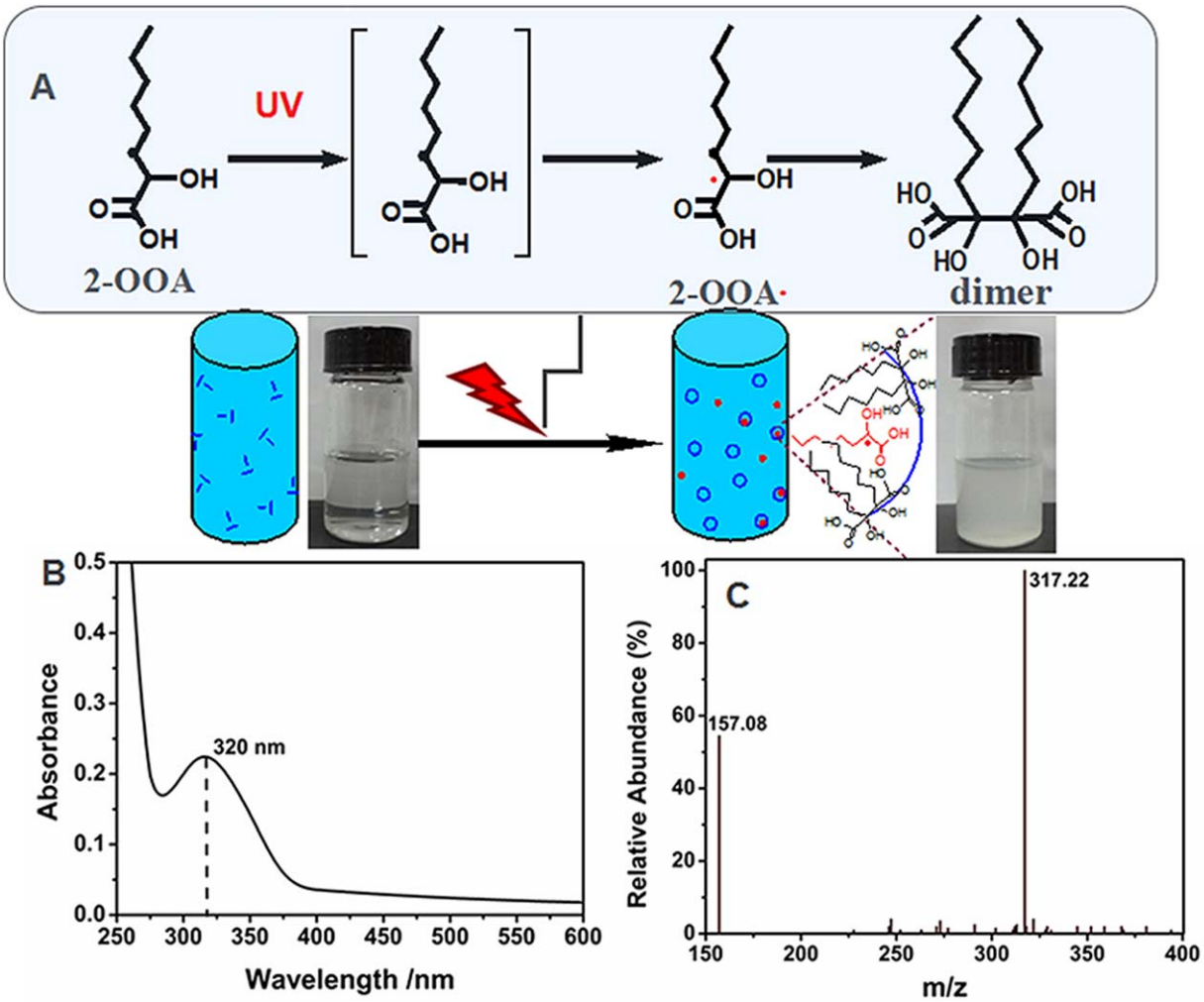

Figure 1. (A) Schematic process of the 2-OOA self-polymerized dimer. (B) UV–vis curve of a 2-OOA aqueous solution. (C) MS spectrum of 2-OOA under UV light irradiation. [Color figure can be viewed in the online issue, which is available at wileyonlinelibrary.com.]

only by the addition of 0.1054 g (0.625 mmol) of TFEMA and 0.0745 g (0.503 mmol) of 4-VPBA monomers with the 2-OOA photoinitiator in the same way as the procedure for the synthesis of the poly(MAAM-*co*-MAPEG-*co*-VPBA) copolymer.

Preparation of the Poly(MAAM-*co*-MAPEG-*co*-VPBA) and Insulin-Loaded Micelles

The poly(MAAM-*co*-MAPEG-*co*-VPBA) and insulin-loaded micelles were prepared by the dialysis method. An amount of 0.2 g of poly(MAAM-*co*-MAPEG-*co*-VPBA) copolymer power was dissolved in 5 mL of tetrahydrofuran with ultrasound treatment. Then, the deionized water was added slowly to the polymer solution until emulsion occurred. The emulsion was dialyzed against deionized water for 3 days with a dialysis bag (MWCO = 3500 Da). The polymer micelles were obtained as a light yellow solid by lyophilization. For the preparation of insulin-loaded micelles, 0.1 g of poly(MAAM-*co*-MAPEG-*co*-VPBA) micelles were dispersed in aqueous solution and sonicated for 10 min. An amount of 5 mg of insulin dissolved in water and ethanol (1:3 v/v) mixture was added to the previous solution slowly until emulsion appeared under strong magnetic stirring. The insulin-loaded micelle solution was dialyzed against deionized water in a dialysis bag (MWCO = 7000 Da) to remove the unloaded insulin. The insulin entrapment capacity and entrapment efficiency were calculated to be about 84.38 and 11.25%, respectively.

Characterization

The ^{1}H-NMR spectra were recorded on a Bruker AV 400-MHz spectrometer with $CDCl_3$ as a solvent and tetramethylsilane as an internal standard. Fourier transform infrared spectra were performed on a Nicolet 5700 instrument with the potassium bromide (KBr) tablet method. Transmission electron microscopy (TEM) measurements were recorded on a JEM-2100 instrument (Japan) with an accelerating voltage of 120 kV. Dynamic light scattering (DLS) measurements were performed in an aqueous solution with a Malvern Zetasizer Nano Series instrument. Mass spectrometry (MS) was performed with a mass spectrometer (5973I, Agilent Technologies). Ultraviolet–visible (UV–vis) spectra were recorded on a Hitachi U3900H instrument.

The fluorescence spectrum measurement of the obtain fluorescence polymer was monitored with an F-4500 fluorescence spectrophotometer (Hitachi, Japan). The emission spectrum of the

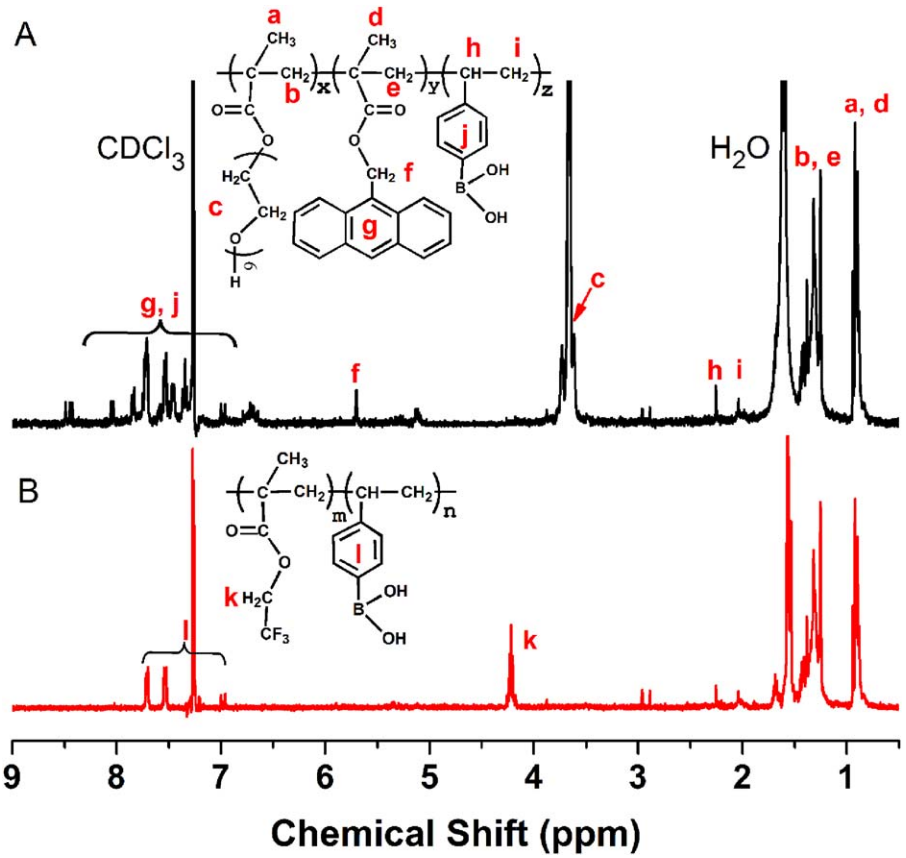

Figure 2. ^{1}H-NMR spectra of the (A) poly(MAAM-*co*-MAPEG-*co*-VPBA) and (B) poly(TFEMA-*co*-VPBA) copolymers. [Color figure can be viewed in the online issue, which is available at wileyonlinelibrary.com.]

fluorescence copolymer aqueous solution (1×10^{-3} wt %) was scanned from 200 to 500 nm at an excitation wavelength of 252 nm.

The confocal laser scanning microscopy (CLSM) measurement of the fluorescence polymer solution was performed with an FV1000 confocal system (Olympus, Japan). The experiment was carried out by the placement of a fluorescence copolymer solution (10 μL) on a cover glass. The image acquisition was performed immediately. Inverted fluorescence microscopy measurement of the fluorescence polymer solution was performed with a TE2000U instrument (Nikon, Japan) with blue and green light as irradiation light sources.

The influence of the glucose on the hydrodynamic radius of the fluorescence polymer micelles were studied by DLS at different glucose concentrations from 0 to 11 mg/mL at room temperature. The stability of the as-prepared micelles was estimated in 100% fetal bovine serum (FBS) at 37°C. The diameter change was measured by DLS over 48 h.

The insulin release from the insulin-loaded micelles was evaluated with different glucose concentrations (0, 2, and 5 mg/mL) in PBS at pH 7.4 *in vitro*. Typically, 15 mg of insulin-loaded micelles solid was first dispersed in 5 mL of PBS and subsequently introduced into a dialysis bag (MWCO = 7000 Da). The release experiment was initiated by the placement of the end-sealed dialysis bag into 150 mL of PBS at 37°C with continuous shaking at 80 rpm. At a predetermined time point, the same amount of release medium was taken out and replaced by the same volume of fresh PBS. The drug concentration was detected by UV–vis spectrophotometry absorbance at 235 nm.

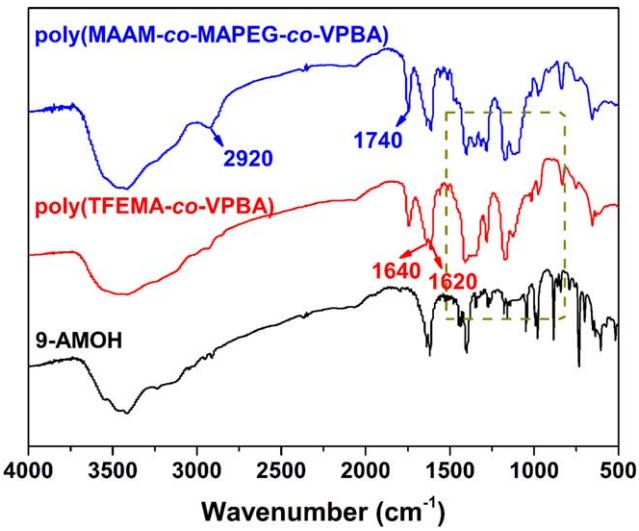

Figure 3. Fourier transform infrared spectra of the poly(MAAM-*co*-MAPEG-*co*-VPBA) and poly(TFEMA-*co*-VPBA) copolymers and the 9-AMOH monomer. [Color figure can be viewed in the online issue, which is available at wileyonlinelibrary.com.]

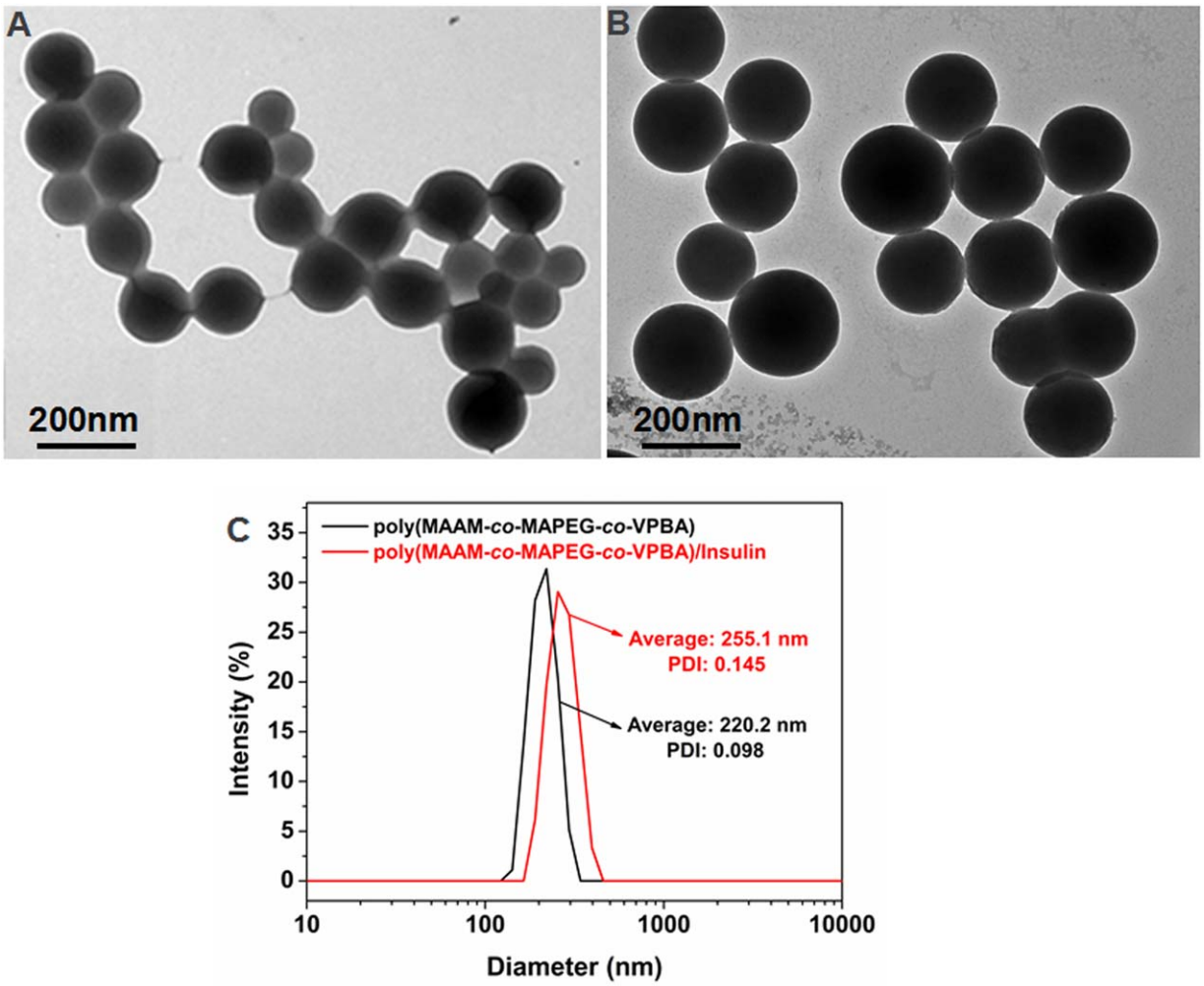

Figure 4. TEM images of the (A) poly(MAAM-*co*-MAPEG-*co*-VPBA) and (B) insulin-loaded micelles. (C) Particle size distribution curves of poly(MAAM-*co*-MAPEG-*co*-VPBA) and the insulin-loaded micelles. [Color figure can be viewed in the online issue, which is available at wileyonlinelibrary.com.]

The relative cytotoxicity was assessed by an MTT viability assay against A549 cells. A549 cells were selected and seeded onto 96-well plates at a density of 5000 cells per well with 100 μL of growth medium. The preprepared micelles solutions were diluted to give a range of final concentration from 0 to 160 μg/mL with culture medium. The plates were maintained in the incubator for 24 and 48 h, respectively. The cell viability was calculated with the following equation:

$$\text{Cell viability } (\%) = \frac{A_{\text{sample}}}{A_{\text{control}}} \times 100$$

where A_{sample} and A_{control} are the absorbances of the sample and control wells measured on a SpectraMax Series microplate reader at 490 nm, respectively.

RESULTS AND DISCUSSION

2-OOA Self-Polymerized Dimer under UV Irradiation

2-OOA is a water-soluble ketone photoinitiator and emulsifier derived from its special structure, which contains a hydrophobic segment (eight-carbon) and pendant hydrophilic groups. Figure 1(A) shows the photographs of a transparent 2-OOA solution (1 mg/mL) before photolysis. After UV irradiation, the color of the 2-OOA aqueous solution became milky; this suggested the formation of micelles due to the 2-OOA photolysis. Under UV light irradiation, 2-OOA absorbed light through its carbonyl chromophore with a maximum absorption wavelength at 320 nm [Figure 1(B)]; this resulted in the production of radicals. The photolysis of 2-OOA under UV irradiation was confirmed by MS analysis. As shown in Figure 1(C), two different ion peaks [mass-to-charge ratio (m/z) = 157.08 and 317.22] were observed under the assistance of UV irradiation; they were assigned to 2-OOA (m/z = 157.08) and OOA–OOA (m/z = 317.22) dimer molecular structures. 2-OOA was reversibly hydrated in an aqueous solution. In aqueous solution, some 2-OOA existed in its keto form, with the majority existing as its gem diol.[33] The keto form contained a UV chromophore, which could be excited in the near-UV state to induce photolysis to form the radical intermediate 2-OOA·. Some radicals reacted with each other to form dimer molecules. These formed dimer molecules were further self-assembled into micelles. The dimer molecules contained hydrophobic alkane ketones and hydrophilic carboxyl groups. They acted as the surfactant or emulsifier to form micelles in solution. The free radicals were dissociated in solution to initiate the polymerization of monomers.[34]

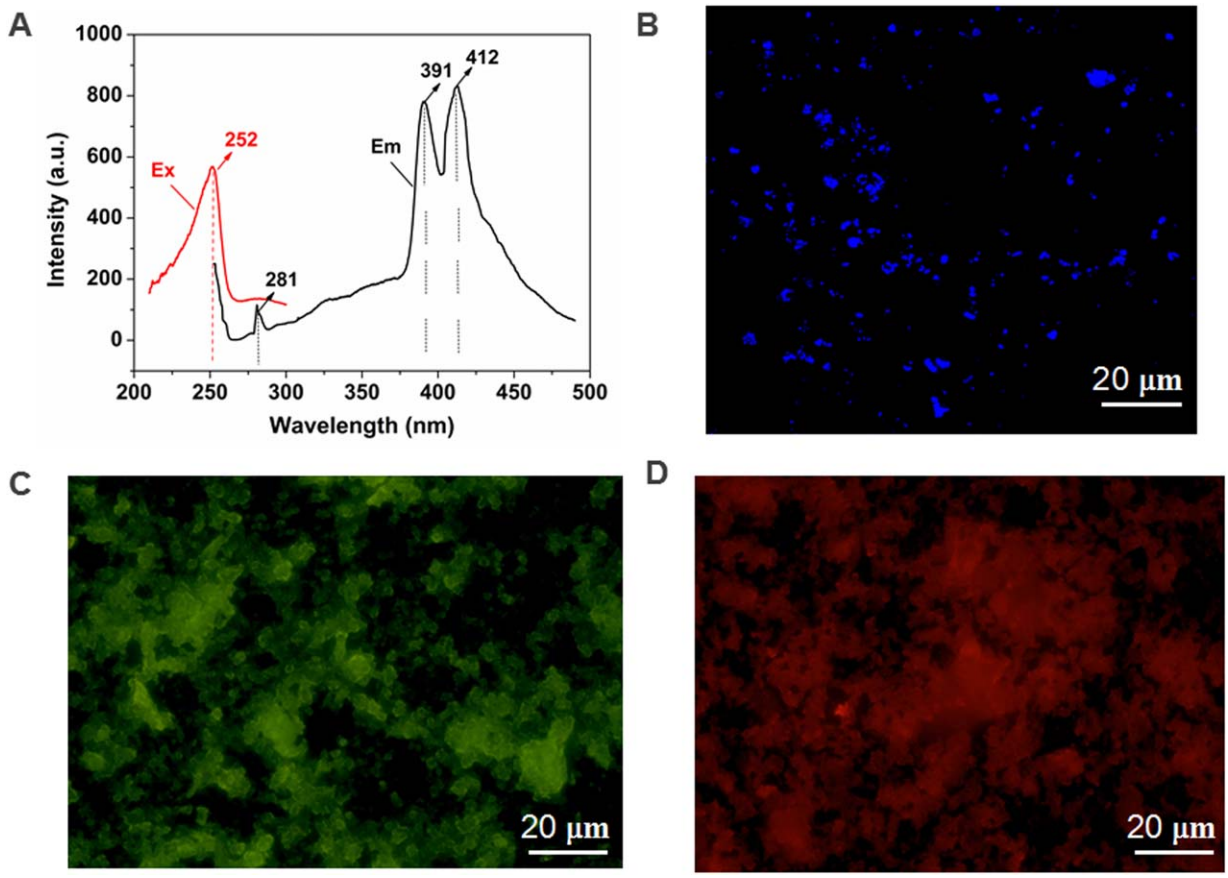

Figure 5. (A) Fluorescence excitation and emission spectra and (B) CLSM image of a poly(MAAM-*co*-MAPEG-*co*-VPBA) solution excited at 408 nm. Inverted fluorescence microscopy images of fluorescence micelles under (C) blue and (D) green light irradiation. [Color figure can be viewed in the online issue, which is available at wileyonlinelibrary.com.]

Synthesis of the Poly(MAAM-*co*-MAPEG-*co*-VPBA) Copolymer

^{1}H-NMR spectroscopy was used to characterize the structure of the poly(MAAM-*co*-MAPEG-*co*-VPBA) copolymer prepared by a one-pot method combination of photoinitiated polymerization and enzymatic transesterification. For the comparison, the poly(TFEMA-*co*-VPBA) copolymer obtained by photopolymerization with and without enzymatic transesterification was synthesized and used to confirm the enzymatic transesterification results. As shown in Figure 2, peaks at 7.00–7.72 ppm were observed and were assigned to the phenyl protons from the poly(TFEMA-*co*-VPBA) copolymer. However, in the case of the poly(MAAM-*co*-MAPEG-*co*-VPBA) copolymer, peaks at 7.00–8.51 ppm were observed and were attributed to the phenyl protons and anthracene protons. The difference was due to anthracycline, which improved the electron densities of the protons through π–π interactions. This led to their signals being shifted to higher magnetic fields.[35] This suggests that the fluorophore segments were successfully introduced into the polymer chains. The strong protons peaks at 3.65–3.74 ppm were assigned to PEG segment protons. By comparing ^{1}H-NMR results of two copolymers, we observed that the proton peak around 4.22 ppm nearly disappeared in poly(MAAM-*co*-MAPEG-*co*-VPBA). The proton peak was attributed to the ethyl ester protons of poly(trifluoroethyl methacrylate) (poly(TFEMA));[36] this indicated that the transesterification reaction was nearly complete. On the basis of the integral value of trifluroethyl segment protons (—CH_2CF_3—) at 4.22 ppm and phenyl protons at 7.00–7.72 ppm, the ratio of the degrees of polymerization (*m* and *n*) of poly(TFEMA-*co*-VPBA) were calculated to be around 1.65:1.00. Similarly, combined with the integral values of the PEG segment protons (—CH_2 CH_2—) at 3.65–3.74 ppm, the methylene (—CH_2—) protons at 5.70 ppm, and the phenyl and anthracene protons at 7.00–8.51 ppm, the calculated ratio of the degree of polymerization of poly(MAAM-*co*-MAPEG-*co*-VPBA) was $x/y/z = 1.49{:}1.00{:}5.98$. The previous evidence implied that the fluorescent amphiphilic copolymer was successfully synthesized via a photoinitiated polymerization and chemoenzymatic transesterification method.

Figure 3 shows the Fourier transform infrared spectra of the poly(MAAM-*co*-MAPEG-*co*-VPBA) and poly(TFEMA-*co*-VPBA) copolymers and the 9-AMOH monomer. The broad characteristic peak around 2920 cm^{-1} was assigned to the stretching vibrations of —CH_2— in the PEG segments. The sharp peak at 1740 was attributed to the stretching vibrations of the —C=O bond. The neighboring peaks at 1640 and 1620 cm^{-1} were attributed to the phenyl and anthracene skeleton vibrations. These peaks were observed in the resulting copolymer and further indicated that a copolymer with glucose-sensitive and fluorescence functional groups was successfully introduced.

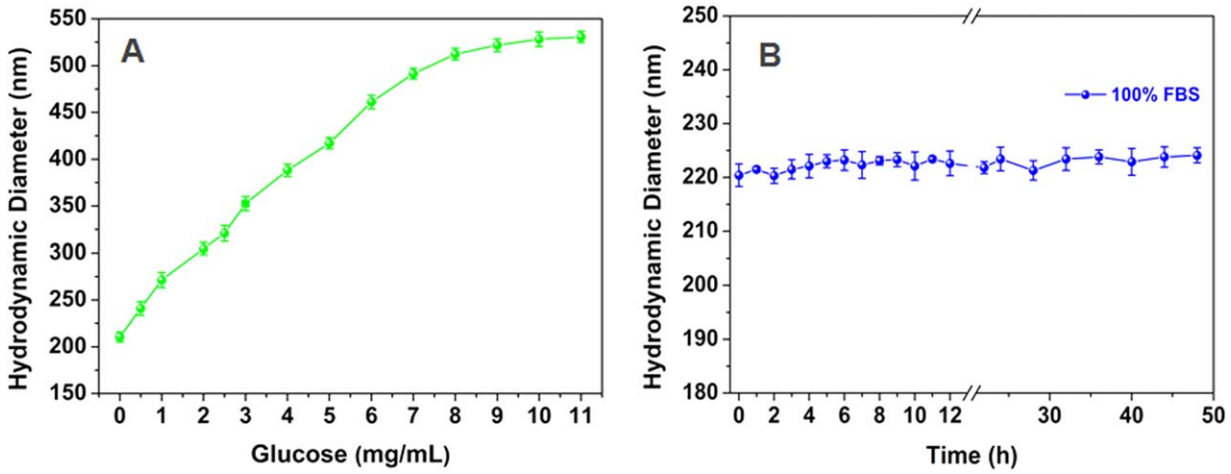

Figure 6. (A) Average hydrodynamic diameter of fluorescence micelles at different glucose concentrations. (B) Stability of fluorescence micelles in 100% FBS at 37°C. [Color figure can be viewed in the online issue, which is available at wileyonlinelibrary.com.]

TEM and Size Distribution (DLS)

The poly(MAAM-*co*-MAPEG-*co*-VPBA) copolymer was further self-assembled into micelles in aqueous solution because of its amphiphilic properties. The transparent and colorless poly (MAAM-*co*-MAPEG-*co*-VPBA)/tetrahydrofuran solution was added dropwise to water under strong magnetic stirring. The color of the mixture solution became milky; this suggested the formation of micelles. The self-assembled particles exhibited a spherical structure with diameters of around 150 nm, as observed from the TEM image in Figure 4(A). Figure 4(B) shows the TEM image of spherical insulin-loaded micelles, and the particle size was about 180–200 nm that larger than that of non-insulin-loaded micelles. The size distribution of as-prepared nanoparticles is further confirmed by DLS. DLS analysis shows that the average diameter of as-prepared copolymer is around 220.2 nm with narrow size distribution, as presented in Figure 4(C). However, the size of the insulin-loaded micelles increased to around 255.1 nm; this was confirmed by DLS analysis and implied the loading of insulin. It was noteworthy that the average diameter determined by DLS was larger than that determined by TEM. This discrepancy was widely considered to be induced by the process of sample preparation and the difference in the investigation methods between DLS and TEM.[37,38]

Fluorescence Properties and Glucose Sensitivity

The fluorescence excitation and emission spectra of the poly (MAAM-*co*-MAPEG-*co*-VPBA) copolymer solution are shown in Figure 5(A). The as-prepared fluorescence polymer micelles exhibited a maximum excitation wavelength at 252 nm. Obviously, three intense fluorescence emission bands at 281, 391, and 412 nm were observed from the fluorescence emission curve on the excitation at 252 nm. Because the polymer micelles had a conjugated structure (π–π) from anthracycline groups, the previous three corresponding fluorescence emission peaks might have been due to the $\pi \rightarrow \pi^*$ electron transition on the excitation wavelength at 252 nm. Fluorescence dyes or labels were visualized with CLSM.[39,40] The blue fluorescence phenomenon was observed clearly by CLSM excited at 408 nm, as shown in Figure 5(B). This result was consistent with blue fluorescence under 365 nm UV irradiation. On the other hand, from the inverted fluorescence microscope image in Figure 5(C), green fluorescence appeared under blue light irradiation. However, under green light irradiation, red fluorescence was observed, as shown in Figure 5(D). Under different irradiation, the emitting fluorescence changed with external excitation wavelength. This was due to the different energy level transitions under different light sources. On the other hand, nonradiation energy transfer could occur and lead to a change in the fluorescence intensity, which caused the fluorescence color to be transformed.[41] Meanwhile, single and composite lights had an important impact on the fluorescence color. The fluorescence emission made it a potentially photoactive material that could be applied for imaging purposes in biological fields.

The glucose sensitivity of the poly(MAAM-*co*-MAPEG-*co*-VPBA) copolymer was investigated by DLS analysis. Phenyl boronic acid (PBA) and its derivatives are known to form covalent hydrophilic glucose–PBA complexes with glucose from the uncharged trigonal planar to the negatively charged tetrahedral. The hydrophilic/hydrophobic balance shifts to a more hydrophobic nature with an increase in the particle size.[42–46] As shown in Figure 6(A), with

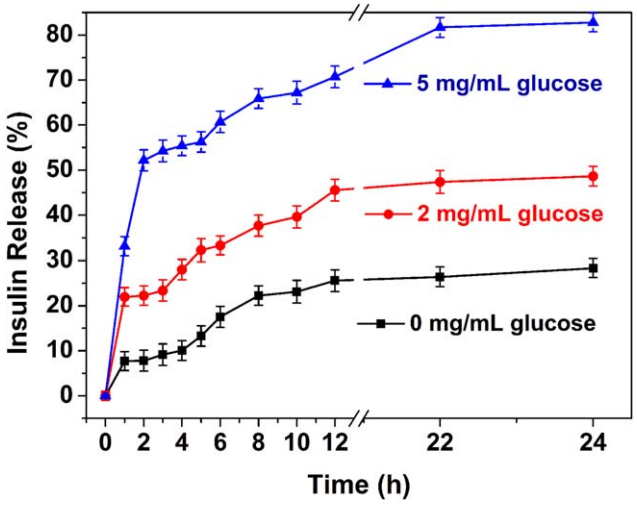

Figure 7. Release of insulin with various glucose concentrations (0, 2, and 5 mg/mL) in PBS at pH 7.4. [Color figure can be viewed in the online issue, which is available at wileyonlinelibrary.com.]

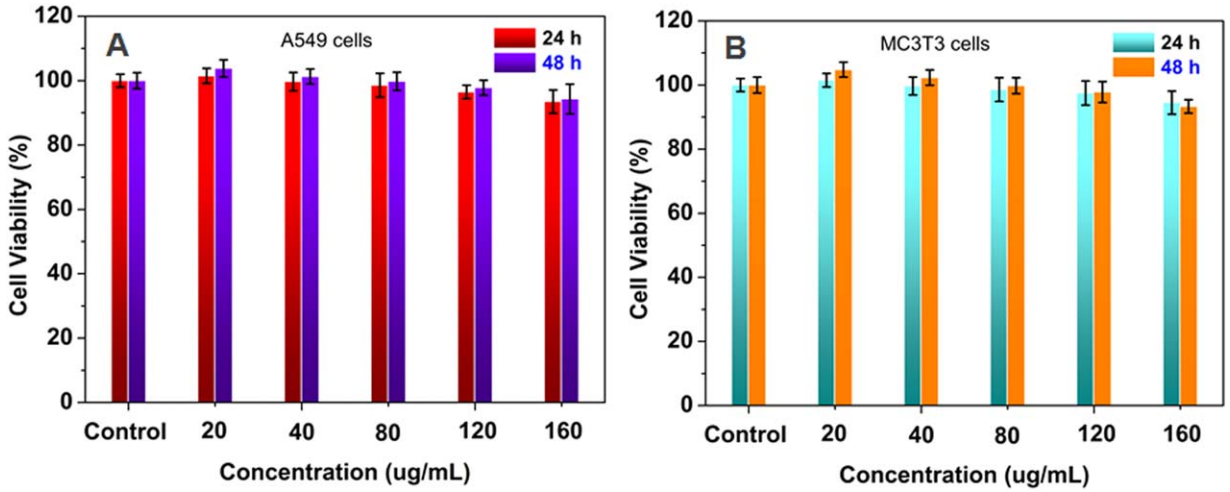

Figure 8. Cell viability of (A) A549 and (B) MC3T3 cells incubated with the as-prepared fluorescence micelles at various concentrations for 24 and 48 h, respectively. The data are presented as the average plus or minus the standard deviation ($n = 5$). [Color figure can be viewed in the online issue, which is available at wileyonlinelibrary.com.]

increasing concentration of glucose (0–8 mg/mL), the size of the micelles exhibited a near-linear dependence on the glucose concentration. When the glucose concentration was 8 mg/mL, the average diameter of particle was 530.6 ± 4.1 nm. However, the average hydrodynamic diameter curve flattened when the glucose concentration was above 8 mg/mL because of the limits of swelling. As drug-delivery vehicles, the micelles underwent complex *in vivo* microenvironmental changes.[47,48] Thus, the micelles had to remain intact in the microenvironment. FBS is usually selected as a model animal protein to study the stability of micelles.[49,50] Herein, the stability of the fluorescence micelles was investigated in the presence of 100% FBS through the measurement of the diameter change. As shown in Figure 6(B), the average hydrodynamic diameters of the micelles remained near their original size with minor deviations even after 48 h of incubation in 100% FBS. This suggested that the drug carriers had excellent stability against protein.

In Vitro Insulin Release

PBA-based polymers have been studied well as a promising material for self-regulated insulin delivery. The as-prepared PBA-based micelles were used to load insulin. Insulin, a hydrophobic drug, was loaded into the he hydrophobic core of the micelles through physical embedding. The glucose-dependent insulin release from the micelles was evaluated *in vitro* with various glucose concentrations in PBS at pH 7.4. As shown in Figure 7, with increasing concentration of glucose, the cumulative release amounts of insulin increased, and the release rate of insulin became faster. All of the release curves showed a quick release of insulin within the first 1 h followed by a sustained release. The cumulative insulin release amounts from the insulin-loaded micelles at glucose concentrations of 0, 2, and 5 mg/mL after 24 h were 28.3, 48.6, and 82.7%, respectively. The increased release amounts of insulin were attributed to the swelling of micelles in the presence of glucose. The results show that the as-synthesized micelles have potential applications in controlled release drug-delivery systems.

Cell Viability

The biocompatibility of a drug-delivery system is very important for practical application. The *in vitro* cytotoxicities of the as-prepared micelles to A549 cells and nomal MC3T3 cells were evaluated with MTT assays. As shown in Figure 8(A), we observed that all of the cell viabilities of the A549 cells were above 90%. After incubation for 48 h, the viability of the cells was around 93.5% even when the concentration of the micelles reached 160 μg/mL. Figure 8(B) shows the low relative cytotoxicity of the as-prepared micelles against nomal MC3T3 cells at given micelle concentrations. The viability of nomal cells still remained above 90%. This indicated the low toxicity and good biocompatibility of the carriers, whether cancer cells or nomal cells. This could have partly been due to the limited use and remaining organic solvents and initiators (or surfactants) during the preparation procedure.[51] Moreover, nonantigenic PEG segments also played an important role in the low toxicity.[52]

CONCLUSIONS

A glucose-sensitive and fluorescent amphiphilic copolymer was synthesized by a combination of photoinitiated polymerization and enzymatic transesterification. The dimer molecules were formed from water-soluble 2-OOA because of its photolysis under UV irradiation. These molecules further acted as the surfactant or emulsifier to form micelles in solution. The free radicals formed by photolysis procedure were dissociated in solution to initiate the polymerization. The glucose-sensitive phenyl boronic acid main chains and fluorescence side groups (9-AMOH) were successfully introduced to endow the micelles with fluorescence. The as-prepared copolymers exhibited excellent glucose sensitivity and stability against protein. Because of the amphiphilic properties of the resulting copolymers, the polymeric micelles were formed by the self-assembly route and used to load insulin. The insulin-release properties exhibited glucose-dependent behavior *in vitro* under physical pH (7.4). In addition, this low-toxicity carrier with good biocompatibility could be a potential candidate for controlled drug release *in vivo*.

ACKNOWLEDGMENTS

This work was financially supported by the National Natural Science Foundation of China (contract grant number 51373155) and the 521 Talents Training Plan of Zhejiang Sci-Tech University.

REFERENCES

1. Gao, W.; Chan, J. M.; Farokhzad, O. C. *Mol. Pharm.* **2010**, *7*, 1913.
2. Hrubý, M.; Koňák, Č.; Ulbrich, K. *J. Controlled Release* **2005**, *103*, 137.
3. Sun, X.; Jiang, G.; Wang, Y.; Xu, Y. *Colloid Polym. Sci.* **2011**, *289*, 677.
4. Cheng, Y.; He, C.; Ding, J.; Xiao, C.; Zhuang, X.; Chen, X. *Biomaterials* **2013**, *34*, 10338.
5. Jin, Q.; Cai, T.; Wang, Y.; Wang, H.; Ji, J. *ACS Macro Lett.* **2014**, *3*, 679.
6. Jochum, F. D.; Theato, P. *Chem. Commun.* **2010**, *46*, 6717.
7. Zhao, L.; Ding, J.; Xiao, C.; He, P.; Tang, Z.; Pang, X.; Zhuang, X.; Chen, X. *J. Mater. Chem.* **2012**, *22*, 12319.
8. Gordijo, C. R.; Koulajian, K.; Shuhendler, A. J.; Bonifacio, L. D.; Huang, H. Y.; Chiang, S.; Ozin, G. A.; Giacca, A.; Wu, X. Y. *Adv. Funct. Mater.* **2011**, *21*, 73.
9. Wang, X.; Jiang, G.; Wei, Z.; Li, X.; Tang, B. *Eur. Polym. J.* **2013**, *49*, 3165.
10. Liu, H.; Zhao, Y.; Dreiss, C. A.; Feng, Y. *Soft Matter* **2014**, *10*, 6387.
11. Brahim, S.; Narinesingh, D.; Guiseppi-Elie, A. *Biosens. Bioelectron.* **2002**, *17*, 973.
12. Qi, W.; Yan, X.; Fei, J.; Wang, A.; Cui, Y.; Li, J. *Biomaterials* **2009**, *30*, 2799.
13. Rösler, A.; Vandermeulen, G. W. M.; Klok, H.-A. *Adv. Drug Delivery Rev.* **2001**, *53*, 95.
14. Zhu, L.; Wu, W.; Zhu, M.-Q.; Han, J. J.; Hurst, J. K.; Li, A. D. Q. *J. Am. Chem. Soc.* **2007**, *129*, 3524.
15. Li, B. K.; Pan, J.; Feng, S.-S.; Wu, A. W.; Pu, K.-Y.; Liu, Y.; Liu, B. *Adv. Funct. Mater.* **2009**, *19*, 3535.
16. Zhang, X.; Wang, S.; Xu, L.; Feng, L.; Ji, Y.; Tao, L.; Li, S.; Wei, Y. *Nanoscale* **2012**, *4*, 5581.
17. Li, K.; Su, Q.; Yuan, W.; Tian, B.; Shen, B.; Li, Y.; Feng, W.; Li, F. *ACS Appl. Mater. Interfaces* **2015**, *7*, 12278.
18. Roy, D.; Sumerlin, B. S. *ACS Macro Lett.* **2012**, *1*, 529.
19. Etrych, T.; Šírová, M.; Starovoytova, L.; Říhová, B.; Ulbrich, K. *Mol. Pharm.* **2010**, *7*, 1015.
20. Yuan, W.; Yuan, J.; Zheng, S.; Hong, X. *Polymer* **2007**, *48*, 2585.
21. Wan, X.; Liu, T.; Liu, S. *Biomacromolecules* **2011**, *12*, 1146.
22. Wang, D.; Tan, J.; Kang, H.; Ma, L.; Jina, X.; Liu, R.; Huang, Y. *Carbohydr. Polym.* **2011**, 84, 195.
23. Siegwart, D. J.; Oh, J. K.; Matyjaszewski, K. *Prog. Polym. Sci.* **2012**, *37*, 18.
24. Wang, X.; Jiang, G.; Li, X.; Tang, B.; Wei, Z.; Mai, C. *Polym. Chem.* **2013**, *4*, 4574.
25. Wang, Y.; Jiang, G.; Zhang, M.; Wang, L.; Wang, R.; Sun, X. *Soft Matter* **2011**, *7*, 5348.
26. Ito, S.; Goseki, R.; Ishizone, T.; Senda, S.; Hirao, A. *Macromolecules* **2013**, *46*, 819.
27. Ito, S.; Goseki, R.; Ishizone, T.; Hirao, A. *Polym. Chem.* **2014**, *5*, 5523.
28. Andrzejewska, E. *Prog. Polym. Sci.* **2001**, *26*, 605.
29. Yagci, Y.; Jockusch, S.; Turro, N. *J. Macromolecules* **2010**, *43*, 6245.
30. Guo, R.; Gao, Y.; Wu, M.; Wang, H. *Polymer* **2013**, *54*, 4940.
31. Huang, Z.; Zhang, X.; Zhang, X.; Fu, C.; Wang, K.; Yuan, J.; Tao, L.; Wei, Y. *Polym. Chem.* **2015**, *4*, 607.
32. Wang, S.; Fu, C.; Zhang, Y.; Tao, L.; Li, S.; Wei, Y. *ACS Macro Lett.* **2012**, *1*, 1224.
33. Rawashdeh, A. M. M.; Thangavel, A.; Sotiriou-Leventis, C.; Leventis, N. *Org. Lett.* **2008**, *10*, 1131.
34. Ning, J.; Kubota, K.; Li, G.; Haraguchi, K. *React. Funct. Polym.* **2013**, *73*, 969.
35. Gan, H.; Liu, H.; Li, Y.; Zhao, Q.; Li, Y.; Wang, S.; Jiu, T.; Wang, N.; He, X.; Yu, D.; Zhu, D. *J. Am. Chem. Soc.* **2005**, *127*, 12452.
36. Fu, C.; Zhu, C.; Wang, S.; Liu, H.; Zhang, Y.; Guo, H.; Tao, L.; Wei, Y. *Polym. Chem.* **2013**, *4*, 264.
37. Jiang, G.; Wang, Y.; Zhang, R.; Wang, R.; Wang, X.; Zhang, M.; Sun, X.; Bao, S.; Wang, T.; Wang, S. *ACS Macro Lett.* **2012**, *1*, 489.
38. Wang, X.; Sun, X.; Jiang, G.; Wang, R.; Hu, R.; Xi, X.; Zhou, Y.; Wang, S.; Wang, T. *J. Appl. Polym. Sci.* **2013**, *128*, 3289.
39. Li, W.; Zhang, W.; Yang, X.; Xie, Z.; Jing, X. *J. Appl. Polym. Sci.* **2014**, *131*, 40433.
40. Li, L.; Jiang, G.; Du, X.; Chen, H.; Liu, Y.; Huang, Q.; Kong, X.; Yao, J. *RSC Adv.* **2015**, *5*, 75766.
41. Guven, N.; Camurlu, P. *Polymer* **2015**, *73*, 122.
42. Ma, R.; Yang, H.; Li, Z.; Liu, G.; Sun, X.; Liu, X.; An, Y.; Shi, L. *Biomacromolecules* **2012**, *13*, 3409.
43. Watahiki, R.; Sato, K.; Suwa, K.; Niina, S.; Egawa, Y.; Seki, T.; Anzai, J.-I. *J. Mater. Chem. B* **2014**, *2*, 5809.
44. Cheng, F.; Jäkle, F. *Polym. Chem.* **2011**, *2*, 2122.
45. Giacomelli, C.; Schmidt, V.; Borsali, R. *Macromolecules* **2007**, *40*, 2148.
46. Du, X.; Jiang, G.; Li, L.; Liu, Y.; Chen, H.; Huang, Q. *Colloid Polym. Sci.* **2015**, *293*, 2129.
47. Owena, S. C.; Chan, D. P. Y.; Shoichet, M. S. *Nano Today* **2012**, *7*, 53.
48. Bae, Y.; Fukushima, S.; Harada, A.; Kataoka, K. *Angew. Chem. Int. Ed.* **2003**, *42*, 4640.
49. Jiang, G.; Jiang, T.; Chen, H.; Li, L.; Liu, Y.; Zhou, H.; Feng, Y.; Zhou, J. *Colloid Polym. Sci.* **2015**, *293*, 209.
50. Opanasopit, P.; Yokoyama, M.; Watanabe, M.; Kawano, K.; Maitani, Y.; Okano, T. *J. Controlled Release* **2005**, *104*, 313.
51. Jiang, G.; Du, X.; Wei, Z.; Jiang, T.; Zhou, H.; Qiu, Z. *Eur. Polym. J.* **2014**, *60*, 33.
52. Puri, M.; Kaur, I.; Perugini, M. A.; Gupta, R. C. *Drug Discovery Today* **2012**, *17*, 774.